Technologies and Materials for Renewable Energy, Environment & Sustainability

Numerical Simulation of the Aeroacoustic Coupling of a Turbulent Plane Jet Impinging on a Slotted Plate

AIPCP25-CF-TMREES2025-00034 | Article

Submitted on: 09-12-2025

Numerical Simulation of the Aeroacoustic Coupling of a Turbulent Plane Jet Impinging on a Slotted Plate

Mohammad Issa[1, b)], Nour Eldin Afyouni [2, c)], Kamel Abed-Meraim[3, d)], Marwan Alkheir[1, 4, e)], Hassan Assoum[3, 5, a)] and Anas Sakout [3, f)]

[1] *Lebanese University, Faculty of sciences, Tripoli, Lebanon*
[2] *CESI, Faculty of Engineering, La Rochelle, France*
[3] *LASIE UMR CNRS 7356, La Rochelle University, La Rochelle, France*
[4] *Arab Open University, Tripoli, Lebanon*
[5] *Beirut Arab University, Mechanical Engineering Department, Beirut, Lebanon*

[a)] *Corresponding author: h.assoum@bau.edu.lb*
[b)]*issabadermohammad02@gmail.com*
[c)]*nour.afyouni@gmail.com*
[d)]*kabedmer@univ-lr.fr*
[e)]*marwanalkheir@gmail.com*
[f)]*asakout@univ-lr.fr*

Abstract. This study focuses on the numerical simulation of a turbulent flow interacting with a slotted plate, with the aim of analyzing the aeroacoustic coupling mechanisms responsible for the generation of self-sustained tones. Based on a reference experiment conducted, an unsteady two-dimensional simulation was performed, employing the Detached Eddy Simulation (DES) model to accurately capture the vortex structures. Numerical results at Reynolds numbers 4700 and 4800 show a symmetric behavior in the simulation, unlike the experiment which reveals a transition to antisymmetric behavior at 4800. Acoustics level simulation enabled the detection of a peak of frequency in the acoustic signal similar to what was obtained by the microphone. Additionally, the simulation allowed the exploration of areas that are experimentally difficult to access near the plate. A correlation between the upstream and downstream velocity fields was also demonstrated, highlighting the coherent structures responsible for the feedback loop. The overall good agreement between simulation and experiment validates the numerical approach for understanding the studied physical phenomena.

INTRODUCTION

Impinging jets play a crucial role in a wide range of industrial and engineering applications because of their ability to achieve high rates of momentum and heat transfer. They are extensively employed in cooling processes of turbine blades, electronic devices, combustion systems, drying technologies, and propulsion applications. Beyond their practical uses, impinging jets present complex flow dynamics that continue to be of fundamental scientific interest, particularly in the field of fluid mechanics and aeroacoustics. One of the most remarkable and intriguing phenomena associated with impinging jets is the generation of self-sustained tones [1–8]. These tones are produced as a result of a strong aeroacoustic feedback loop, in which aerodynamic instabilities within the jet interact with the surrounding acoustic field to form a closed feedback mechanism. This interaction leads to the periodic amplification of certain frequencies without the need for any external excitation. Understanding and controlling this phenomenon is essential not only for improving the performance and efficiency of engineering systems but also for mitigating unwanted noise, enhancing safety, and designing quieter and more sustainable technologies. Several theoretical models have been proposed to explain the origin of this aeroacoustic phenomenon. Lighthill's acoustic analogy established a fundamental relationship between jet velocity and acoustic power[9,10] while the works of Powell[11] and Howe[12] highlighted the critical role of the interaction between vorticity and the acoustic velocity field. They demonstrated that energy transfer occurs when the alignment and phase conditions between these two components are satisfied, leading to the amplification of sound waves. Additionally, Rockwell and Naudascher[13] emphasized that such self-sustained oscillations arise naturally from the interaction of the jet with solid structures, giving rise to tonal emissions that characterize many impinging flow systems. A particularly interesting configuration in this context is that of a plane turbulent jet impinging on a slotted plate. In such a system, the shear layer of the jet interacts with the slot edges, generating coherent vortex structures that periodically shed and couple with the acoustic field. Depending on flow

parameters such as the Reynolds number and geometric configuration, the flow may exhibit different regimes, transitioning from symmetric to antisymmetric vortex shedding patterns. These flow regimes strongly influence the tonal characteristics of the resulting acoustic field and are key to understanding the nature of aeroacoustic coupling.

The study of such phenomena has been actively investigated, with numerous experimental and theoretical contributions that have advanced our understanding of flow-acoustic interactions[14]. This work fits naturally within that scientific framework and represents a continuation of the laboratory's long-standing efforts. It also contributes to the development of numerical tools and methodologies that complement experimental approaches, allowing researchers to access flow regions and physical details that are often difficult or impossible to measure experimentally.

The numerical work presented in this study is closely linked to a well-established experimental investigation performed under comparable conditions and used as the main reference for validation. In this experiment, a turbulent plane jet impinging on the same slotted plate were studied at Reynolds numbers of 4700 and 4800 values chosen within the range typical of flows in confined environments. Despite their proximity, these two cases exhibited significantly different acoustic behaviors, with one producing a strong, high-pitched self-sustained tone and the other remaining relatively quiet. The experimental platform, specifically designed for this study, includes a controlled air supply, a stabilization chamber, honeycomb grids, and a polynomial convergent to generate a subsonic planar jet that impacts an aluminum slotted plate with an impact distance of L = 4 cm. Velocity fields were measured using SPIV, while acoustic pressure spectra were recorded with microphones. The results revealed strong correlations between vortex dynamics and acoustic emission, as well as sudden changes in tonal behavior associated with the reorganization of large-scale coherent structures. These experimental observations provide a comprehensive and reliable database against which the present numerical simulations are validated. In this context, the present work aims to provide a comprehensive numerical investigation of a plane turbulent jet impinging on a slotted plate, focusing on the underlying aeroacoustic coupling mechanisms responsible for the generation of self-sustained tones. Based on previous studies, an unsteady two-dimensional simulation is conducted, employing the Detached Eddy Simulation (DES) model to accurately capture vortex structures and flow dynamics. Through this numerical approach, the study seeks to reproduce the experimental observations, analyze the interaction between vortex structures and the acoustic field, and shed light on the mechanisms that govern the feedback loop. Furthermore, the simulation makes it possible to explore areas that are challenging to access experimentally, providing valuable physical insights into the behavior of the flow and its acoustic response, while also enriching the physical interpretation of the observed phenomena.

NUMERICAL METHODOLOGY

Domain and Geometry

The numerical simulation was designed to replicate the experimental setup illustrated in Fig.1a as closely as possible in order to capture the essential physical mechanisms governing the interaction between the jet and the slotted plate. The objective was to construct a computational domain that accurately represents both the impinging jet and the downstream flow generated by this interaction. Based on previous experimental observations[15], the third velocity component was found to have a negligible influence on the overall flow dynamics. Therefore, a two-dimensional (2D) model in the XY plane, as shown in Fig.1b was selected to significantly reduce the computational cost while maintaining the physical accuracy of the studied phenomenon.

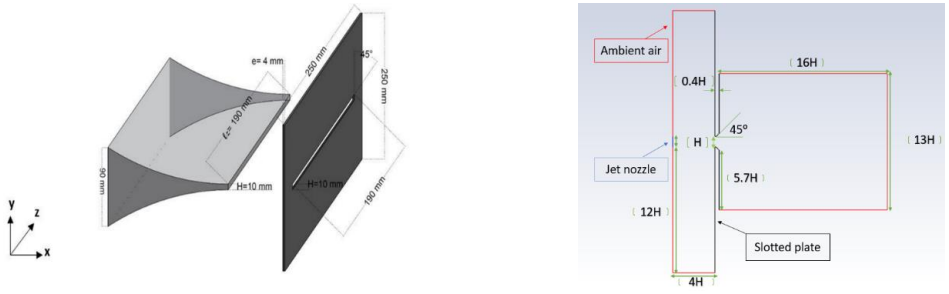

(a) (b)

FIGURE 1. (a) Geometry of the experimental configuration, (b) Geometry of the numerical simulation domain.

To avoid numerical artifacts caused by boundary conditions and ensure that they do not influence the main region of interest, the domain size was intentionally extended beyond the immediate interaction zone. Although the primary interaction occurs around 4H downstream of the slot, the domain length was extended to 16H in the streamwise direction to allow the flow to fully develop and to capture the acoustic feedback mechanisms. Similarly, the vertical dimension of the domain, theoretically requiring only 4H, was extended to 12H to ensure numerical stability and minimize boundary effects[16].

The nozzle exit was designed with a height H = 10 mm identical to the slot opening of the plate to maintain consistent jet characteristics. The distance between the nozzle exit and the plate was set to 4H, matching the experimental configuration. Additionally, the downstream edge of the slotted plate was beveled at a 45° angle to promote the formation of coherent vortical structures and enhance acoustic source generation.

Mesh Generation

An unstructured mesh was generated to accurately resolve the shear layers, boundary layers, and vortex formation regions while maintaining computational efficiency. The domain was divided into two regions based on the expected flow gradients: a highly refined mesh in the near-jet region, the shear layer, and around the impingement area. This ensured accurate resolution of vortex dynamics and acoustic feedback mechanisms, and a coarser mesh further away from the main flow region, where gradients are weaker and high resolution is not required, is shown in Fig.2a.

A total of 20 inflation layers were applied near the wall with a growth rate of 1.1 to properly resolve the boundary layer, as presented in Fig.2b. The thickness of the first cell was set to 0.028 mm, corresponding to a near-wall non-dimensional distance $y^+ \approx 1$, which satisfies the requirements of the turbulence modeling[16].

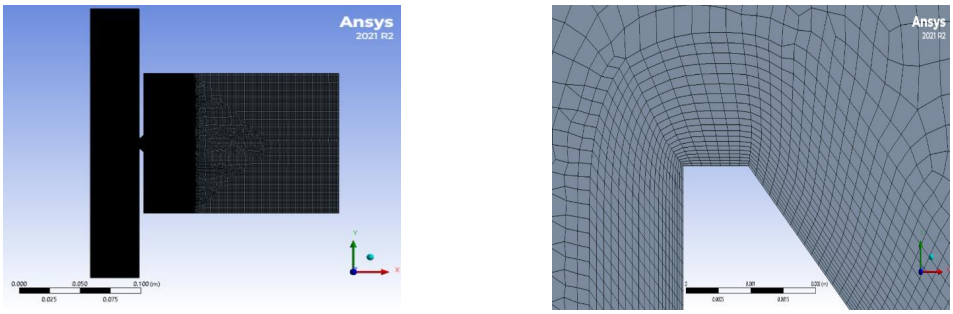

(a) (b)

FIGURE 2. (a) Global view of the computational domain showing the two mesh regions, (b) Zoomed view near the wall illustrating the inflation layers used to accurately resolve the boundary layer.

A mesh independence study was carried out to ensure that the numerical results were not sensitive to grid resolution. Multiple mesh densities were tested, and variations in key flow quantities (such as velocity profiles, pressure fluctuations, and dominant acoustic frequencies) were monitored. The results confirmed that the chosen grid resolution provides a good balance between computational cost and numerical accuracy.

Simulation Strategy and Numerical Setup

The simulations were performed using the ANSYS Fluent solver under an unsteady, incompressible, pressure-based formulation. This approach is well suited to the subsonic flow conditions considered here (Mach ≈ 0.1) and to the Reynolds numbers under investigation (Re = 4700 and Re = 4800). The two-dimensional, time-dependent Navier–Stokes equations, together with the continuity equation, were solved to capture the flow dynamics and their aeroacoustic interactions with the slotted plate.

The computational setup was designed to closely replicate the experimental configuration, particularly in terms of boundary conditions. At the inlet, a uniform velocity of 7.1 m/s was imposed, corresponding to Re = 4700 (7.21 m/s for Re = 4800), ensuring consistency with the reference experiment. The turbulence intensity was fixed at 2%, representing realistic flow conditions at the inlet, and the hydraulic diameter was set to 0.01 m to correctly define the turbulence length scale. The temperature was maintained at 294.15 K, matching ambient experimental conditions. All

solid walls were treated as stationary with a no-slip condition, and a zero-heat-flux boundary was imposed to represent adiabatic walls, as in the experimental setup. At the outlet, an atmospheric pressure was applied to provide a stable reference for the flow field and to avoid spurious reflections that could contaminate the acoustic field.

The simulation process was divided into two main stages. First, a steady-state simulation was conducted to provide a physically meaningful initial condition and ensure that the flow reached a quasi-equilibrium state before transitioning to the unsteady regime[16]. Once this state was achieved, a transient simulation was launched to capture the development and evolution of unsteady vortical structures and their interaction with the acoustic field. The time step used in the transient simulation was 0.0001 s, which is sufficiently small to resolve the key hydrodynamic and acoustic time scales. The total simulation time was 1.3 s, with the first 0.3 s used for flow stabilization and the remaining 1.0 s dedicated to collecting data for analysis.

The coupling between pressure and velocity fields was handled using the Coupled scheme for improved stability and convergence. Pressure interpolation was performed using the PRESTO scheme to accurately capture strong pressure gradients, particularly near the impingement zone. Spatial discretization of the convection terms was achieved with a second-order upwind scheme to minimize numerical diffusion, while a second-order implicit scheme was used for time discretization to resolve unsteady phenomena over long simulation times.

Turbulence modeling was carried out using the Delayed Detached Eddy Simulation (DDES) approach in combination with the k–ω SST model. This hybrid RANS–LES method uses RANS modeling near walls and LES-like resolution in separated and shear-layer regions[16], making it ideal for resolving large-scale coherent structures, which are the primary drivers of the aeroacoustic feedback loop.

To extract dynamic flow and acoustic data, the Data Sampling for Time Statistics option was activated during the transient simulations. Instantaneous velocity fields and time histories were recorded at several probe locations chosen to match those used in the reference experiment. These data were used to analyze the temporal evolution of the flow and to perform spectral analysis.

The acoustic field was analyzed using the Ffowcs Williams–Hawkings (FW-H) analogy, with the slotted plate defined as the acoustic source surface. Virtual receivers were placed at the same locations as in the experiment to allow direct comparison between numerical and experimental results. Spectral analysis was performed by applying a Fast Fourier Transform (FFT) to the velocity signals obtained from these probes. This made it possible to identify the dominant frequencies associated with vortex shedding and aeroacoustic coupling, including the fundamental self-sustained tone and its harmonics.

The combined use of advanced turbulence modeling, accurate temporal and spatial discretization, and carefully defined boundary conditions provides a robust numerical framework capable of reproducing the essential physical features of the jet–plate interaction. This methodology allows for a detailed examination of the aerodynamic–acoustic coupling mechanisms and serves as a reliable tool for comparing simulation results with experimental observations.

RESULTS AND VALIDATION

In this section, the numerical results obtained from the CFD simulations are presented and compared directly with the experimental measurements. The objective is to assess the capability of the simulation to reproduce the main flow structures, aeroacoustics features, and overall physical phenomena observed in the reference experiment. For each case, simulation and experimental data are presented side by side to allow for a direct and detailed validation.

Mean Velocity Contours (Re = 4700)

The global structure of the mean velocity field obtained from the simulation closely matches that observed experimentally, indicating that the main flow features and the interaction between the jet and the slotted plate are well reproduced. The velocity contours reveal similar jet spreading, impingement behavior, and recirculation zones in both approaches, demonstrating that the numerical model accurately captures the overall dynamics of the flow.

Minor discrepancies are observed, primarily near the plate boundaries, as shown in Fig.3, where the mean velocity contours from both the simulation and the experiment exhibit comparable global behavior. In the experimental results, the region adjacent to the plate is not visible due to laser reflections on the surface, which completely obscure the velocity measurements near the wall. In contrast, the simulation clearly delineates this area, allowing a better visualization of the jet impact and near-wall recirculation. These differences, together with slight deviations in the shear-layer thickness, are mainly attributed to boundary condition effects, differences in spatial resolution, and the idealized nature of the numerical setup compared to the experimental environment.

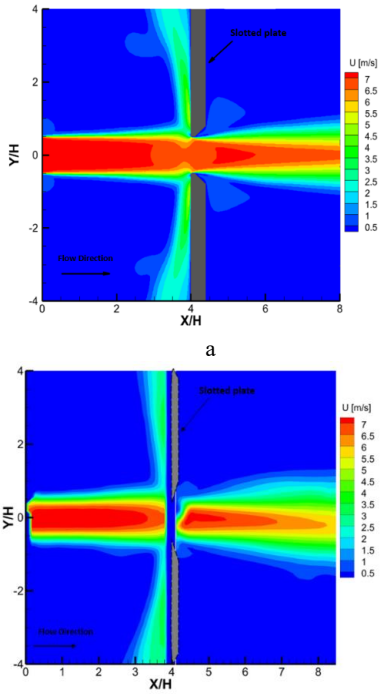

FIGURE 3. (a) Mean Velocity Contour: Simulation , (b) Mean Velocity Contour: Experiment.

Vortex Trajectories and Tourbillon Dynamics (Re = 4700)

Vortex trajectories obtained from the superposition of λ_2 fields show consistent birth, convection, and deviation of coherent structures on both sides of the slot. The spatial organization and symmetry state agree well with the experimental observations, confirming the model's ability to reproduce the dominant vortex dynamics, as shown in Fig.4. In addition to capturing the global behavior, the simulation reveals detailed vortex motion along the plate surface and in regions where experimental measurements were obstructed by optical limitations, such as laser reflections and restricted seeding. This numerical visualization provides valuable insight into the near-wall evolution of coherent structures and their role in the aeroacoustic feedback process areas that remain partially or completely inaccessible in the experimental setup.

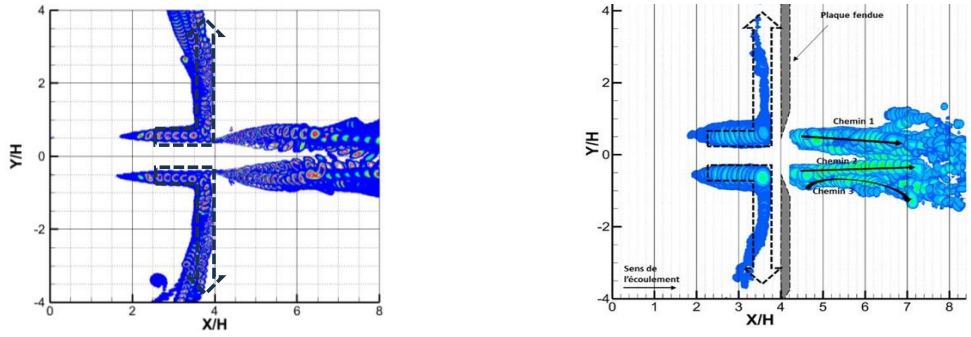

FIGURE 4. (a) Vortex Trajectories: Simulation, (b) Vortex Trajectories : Experiment.

Acoustic Spectra Comparison (Re = 4700)

The acoustic spectra from simulation and experiment agree closely on the dominant tone (202–204 Hz) and its first harmonic; simulated levels are slightly higher (85 dB vs 80 dB). The simulation also reveals two additional tones, later linked to flow mechanisms at 88 Hz and 114 Hz, which are less evident in the experiment, as shown in Fig.5.

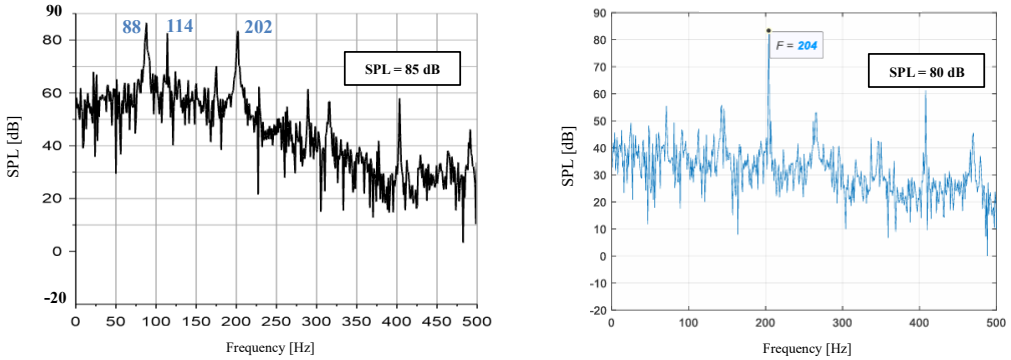

(a) (b)

FIGURE 5. (a) Acoustic Spectra: Simulation, (b) Acoustic Spectra: Experiment.

Dynamic Velocity Spectra at Selected Points (Re = 4700)

To better interpret and correlate the acoustic spectra with the aerodynamic field, the dynamic velocity spectra were analyzed at several probe locations along the flow field to characterize the dominant frequencies associated with vortex shedding and aeroacoustic coupling. The results are summarized below and presented in Fig.6.

At Point A (X/H = 2, Y/H = 0.5), a strong peak at 202 Hz is observed in both simulation and experiment, indicating the presence of periodic vortex shedding upstream. Moving downstream to Point C (X/H = 3.5, Y/H = 0.5), the 202 Hz tone remains dominant, while weaker components may appear depending on the local passage of coherent structures.

At **Point E (X/H = 3.5, Y/H = 3.5)**, located near the wall, the spectral content reveals strong components associated with boundary-layer vortex activity. Because the **U-velocity component** is perpendicular to the dominant wall-parallel convection, it provides an especially suitable measure for identifying these coherent near-wall structures. From this position, a distinct **88 Hz** component is clearly visible in the spectra. This frequency matches the tone observed in the acoustic measurements, confirming that it originates from **near-wall vortex dynamics** and is directly linked to the boundary-layer structures convected along the wall.

Moving downstream to **Point G (X/H = 5, Y/H = 0.5)**—immediately after the slit—the previously identified **202 Hz** tone remains prominent. Its persistence indicates a strong and continuous correlation between the upstream and downstream flow regions, demonstrating that the coherent structures responsible for this tone are preserved as they pass through the slit. Additionally, two secondary spectral components appear: one at **88 Hz**, consistent with wall-guided vortex structures, and another at **114 Hz**, which corresponds to vortex breakdown and destruction as the vortices traverse the slot and interact with the emerging downstream jet. This interaction leads to energy redistribution across different scales, producing new characteristic frequencies associated with shear-layer deformation and vortex pairing processes.

Finally, at **Point K**, located farther downstream in the flow field, the spectra become progressively flatter, and the previously distinct frequency peaks vanish. This flattening indicates the transition to a **fully developed turbulent regime**, where coherent periodic features decay and energy spreads across a wide range of frequencies. The disappearance of sharp tones reflects the loss of organized vortex structures, replaced by broadband turbulence characteristic of a statistically stationary and chaotic flow.

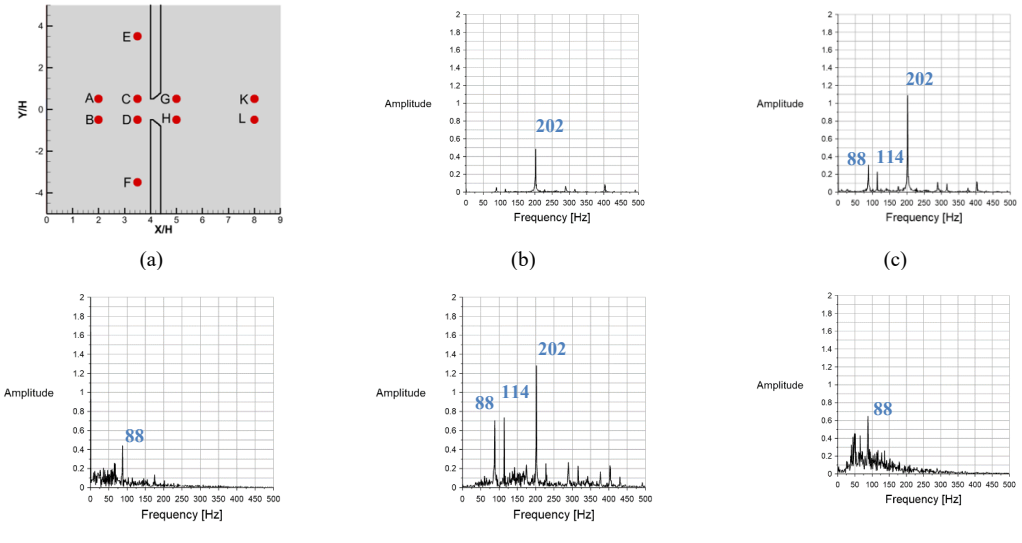

FIGURE 6. (a) Selected Points in Simulation FFT, (b) Point A, (c) Point C, (d) Point E, (e) Point G, (f) Point K.

Regime Continuity and Aeroacoustic Implications (Re = 4800)

At Re = 4800, the simulation remains symmetric, with coherent vortices maintaining their organized pattern, unlike the experiment which shows a transition to an antisymmetric state Fig.7. This confirms that the regime change is not caused solely by the increase in jet velocity but by external excitation present in the experiment and absent in the simulation. As a result, the acoustic spectrum at Re = 4800 remains similar to that at Re = 4700, with slightly higher frequencies, confirming the strong coupling between vortex dynamics and acoustic response.

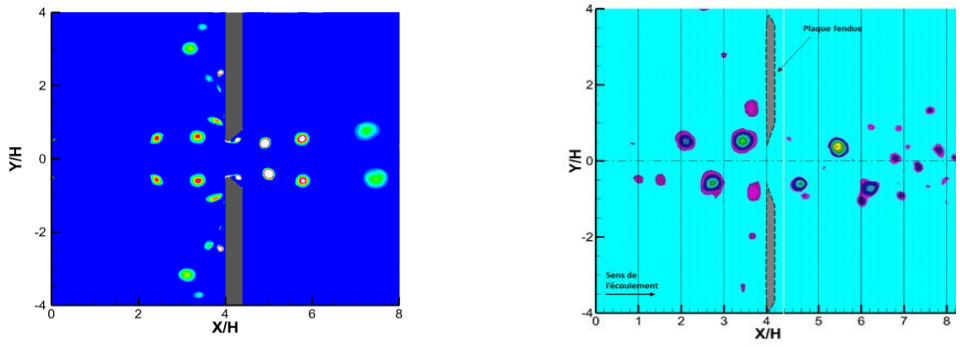

FIGURE 7. (a) Symmetric Regime : Simulation, (b) Antisymmetric Regime : Experiment.

CONCLUSION

The numerical simulation successfully reproduced the main physical phenomena observed experimentally. The mean velocity field and vortex dynamics were well captured, demonstrating that the model accurately represents the essential flow behavior. A strong correlation between upstream and downstream structures was identified, confirming the role of coherent vortices in sustaining the aeroacoustic feedback loop. Acoustically, the simulation predicted a dominant self-sustained tone around 202 Hz, in excellent agreement with the experiment, and revealed its first harmonic and secondary tones linked to additional flow mechanisms. These extra tones, less evident experimentally,

are attributed to idealized numerical conditions and the absence of excitation. The simulation remained symmetric even at Re = 4800, whereas the experiment exhibited a transition to an antisymmetric regime, indicating that external excitation (rather than velocity increase alone) is required to exceed the receptivity threshold and modify the flow behavior. Overall, the numerical approach not only reproduced the experimental results but also provided access to physical details that are experimentally inaccessible. Future work will extend the study to three dimensions to further clarify the aeroacoustic coupling mechanisms.

ACKNOWLEDGMENTS

The authors wish to thank FEDER, the 'Region of Nouvelle Aquitaine' for the financial support of this research.

REFERENCES

1. H.H. Assoum, J. Hamdi, M. Hassan, M. Kheir, K. Abed Meraim, and A. Sakout, "Turbulent Kinetic Energy and Self-Sustaining Tones in an Impinging Jet Using High Speed 3D Tomographic-PIV," Energy Reports **6**, 802–806 (2020) .
2. H.H. Assoum, J. Hamdi, K. Abed-Meraïm, M. El Hassan, M. Ali, and A. Sakout, "Correlation between the acoustic field and the transverse velocity in a plane impinging jet in the presence of self-sustaining tones," Energy Procedia **139**, 391–397 (2017).
3. H. Assoum, J. Hamdi, K. Abed-Meraïm, M. Al Kheir, T. Mrach, L. El Soufi, and A. Sakout, "Spatio-Temporal Changes in the Turbulent Kinetic Energy of a Rectangular Jet Impinging on a Slotted Plate Analyzed with High Speed 3D Tomographic-Particle Image Velocimetry," IJHT **37**(4), 1071–1079 (2019).
4. H.H. Assoum, J. Hamdi, M. Alkheir, K. Abed Meraim, A. Sakout, B. Obeid, and M. El Hassan, "Tomographic Particle Image Velocimetry and Dynamic Mode Decomposition (DMD) in a Rectangular Impinging Jet: Vortex Dynamics and Acoustic Generation," Fluids **6**(12), 429 (2021).
5. B. El Zohbi, H.H. Assoum, M. Alkheir, N. Afyouni, K.A. Meraim, A. Sakout, and M. El Hassan, "Experimental investigation of the Aero-Acoustics of a rectangular jet impinging a slotted plate for different flow regimes," Alexandria Engineering Journal **87**, 404–416 (2024).
6. H.H. Assoum, M. El Kheir, N. Eldin Afyouni, B. El Zohbi, K. Abed Meraim, A. Sakout, and M. El Hassan, "Control of a rectangular impinging jet: Experimental investigation of the flow dynamics and the acoustic field," Alexandria Engineering Journal **79**, 354–365 (2023).
7. N.E. Afyouni, M. Alkheir, H. Assoum, B. El Zohbi, K. Abed-Meraim, A. Sakout, and M. El Hassan, "Effect of a Control Mechanism on the Interaction between a Rectangular Jet and a Slotted Plate: Experimental Study of the Aeroacoustic Field," Fluids **8**(12), 309 (2023).
8. H. Assoum, "Etude expérimentale des couplages entre la dynamique d'un jet qui heurte une plaque fendue et l'émission sonore générée," Ph.D. thesis, La Rochelle University, 2013.
9. M.J. Lighthill, "On sound generated aerodynamically I. General theory," Proc. R. Soc. Lond. A **211**(1107), 564–587 (1952).
10. M.J. Lighthill, "On sound generated aerodynamically II. Turbulence as a source of sound," Proc. R. Soc. Lond. A **222**(1148), 1–32 (1954).
11. A. Powell, "Theory of Vortex Sound," Journal of the Acoustical Society of America **36**(1), 177–195 (1964).
12. M.S. Howe, "Contributions to the theory of aerodynamic sound, with application to excess jet noise and the theory of the flute," J. Fluid Mech. **71**(4), 625–673 (1975).
13. D. Rockwell, and E. Naudascher, "Self-Sustained Oscillations of Impinging Free Shear Layers," Annu. Rev. Fluid Mech. **11**(1), 67–94 (1979).
14. T. Mrach, M. Alkheir, M. El Hassan, H.H. Assoum, E. Etien, and K. Abed-Meraim, "Experimental study of the thermal effect on the acoustic field generated by a jet impinging on a slotted heated plate," Energy Reports **6**, 497–501 (2020).
15. H.H. Assoum, M.E. Hassan, K. Abed-Meraïm, R. Martinuzzi, and A. Sakout, "Experimental analysis of the aero-acoustic coupling in a plane impinging jet on a slotted plate," Fluid Dyn. Res. **45**(4), 045503 (2013).
16. H.K. Versteeg, and W. Malalasekera, *An Introduction to Computational Fluid Dynamics: The Finite Volume Method*, 2nd ed. (Pearson Education Ltd, Harlow, England , New York, 2007).
17. *ANSYS Fluent Theory Guide* (ANSYS, Inc., 2025).